Electronic Supplementary Material (ESI) for New Journal of Chemistry.

Supporting Information

Ultrafine Pt nanoparticles-decorated multi-folded two-dimensional nanosheets for efficient electrocatalytic hydrogen evolution

Yidan Peng, ‡[a] Luping Shen, ‡[a] Haiyan Li, [b] Hongwei He, [a] An Cai, [a] Fengbao Zhang, [ac] Xiaobin Fan, [ac] Wenchao Peng [ac] and Yang Li *[ac]

[a] School of Chemical Engineering and Technology, Tianjin University, Tianjin 300354, P. R. China

E-mail: liyang1895@tju.edu.cn

[b] Daqing Chemical Research Center, Petrochemical Research Institute, PetroChina Company Limited, Heilongjiang Daqing 163714 P. R. China

[c] Institute of Shaoxing Tianjin University, Zhejiang 312300, P. R. China

‡ Yidan Peng and Luping Shen contributed equally to this work.

Characterization

X-ray diffraction (XRD) was used to examine the material's crystalline state on a Smartlab8kW with Cu Kα radiation (λ=1.5418 Å). The microscopic morphology of the catalysts was observed using transmission electron microscopy (TEM) and scanning electron microscopy (SEM), which were tested in this work using a JEM-2100F accelerating voltage of 200 kV and a Hitachi S-4800 microscope accelerating voltage of 3 kV, respectively. X-ray photoelectron spectroscopy (XPS) scans are performed on a Thermo Scientific ESCALAB 250Xi XPS spectrometer to analyze material composition and structure, as well as the valence state of metallic elements. Raman spectroscopy can analyze defects in carbon materials and can also be used to detect metals, using the equipment model Horiba LabRAM HR Evolution. The pore structure and pore size distribution of the catalyst are detected by the Brunauer-Emmett-Teller (BET, BJBuilder SSA-7000) analyzer.

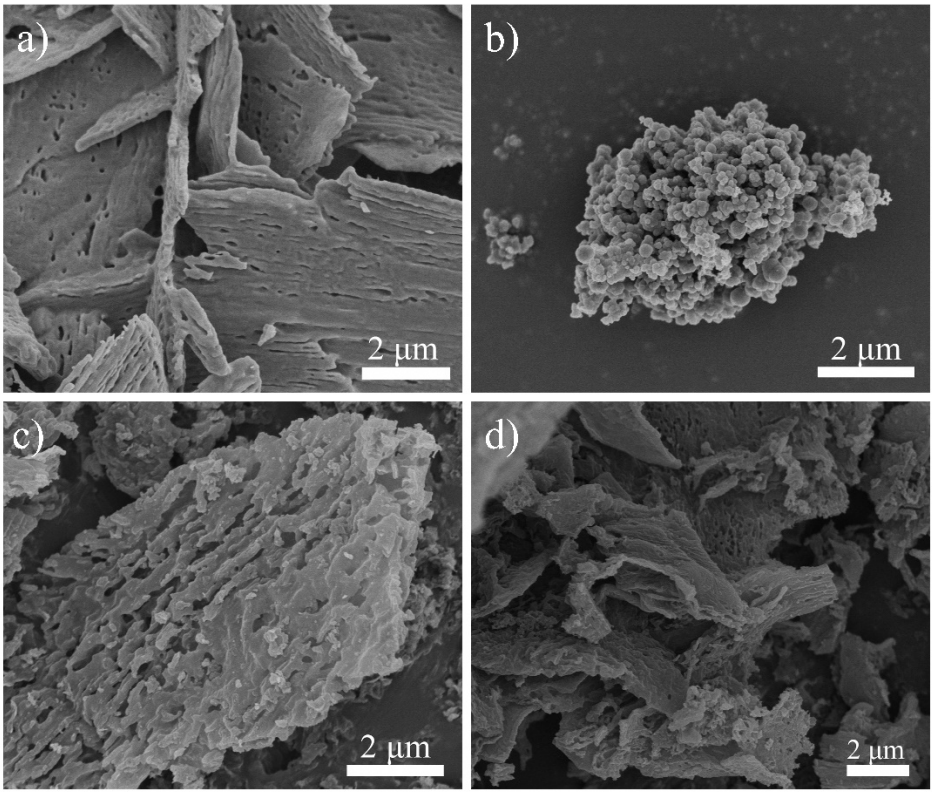

Fig. S1 SEM images of (a) C_3N_4, (b) DA-Pt (1:0), (c) DA-Pt (1:1) and (d) DA-Pt (1:2), respectively.

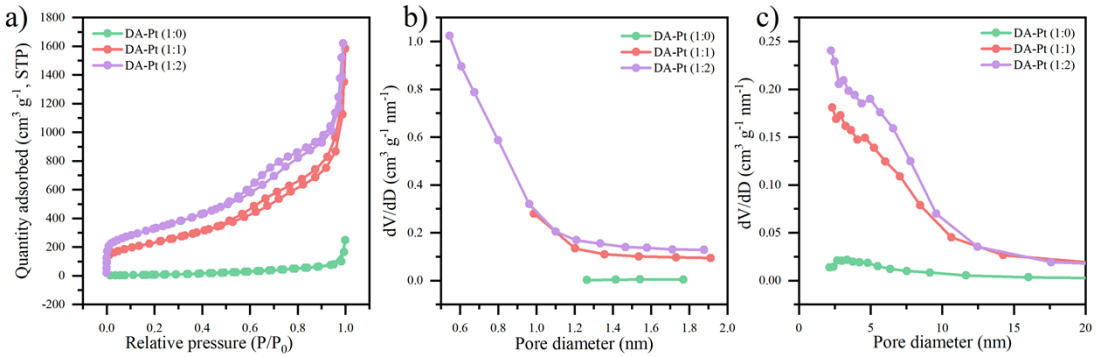

Fig. S2 (a) N_2 adsorption-desorption isotherm, (b) Microporous pore size distribution curves and (c) Mesopore pore size distribution curves of DA-Pt (1:0), DA-Pt (1:1) and DA-Pt (1:2), respectively.

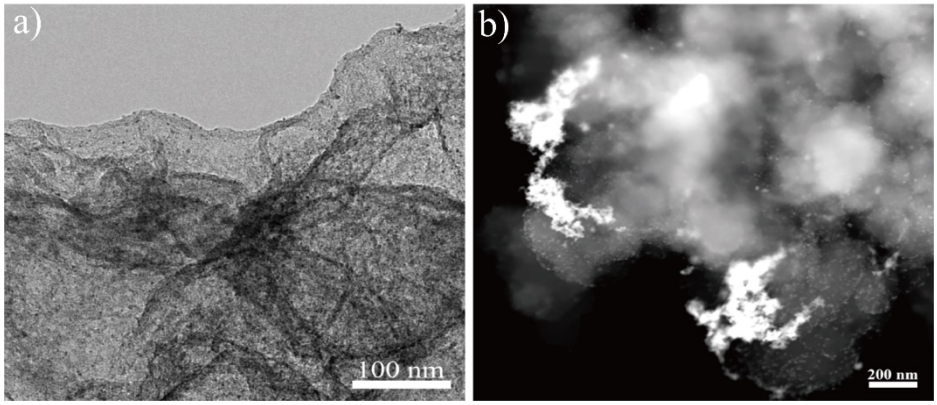

Fig. S3 (a) TEM images of DA-Pt (1:2). (b) HAADF-STEM of DA-Pt (1:0).

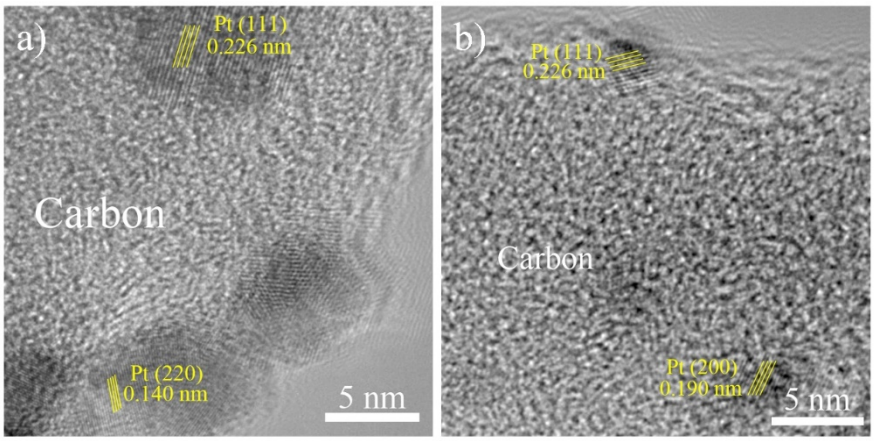

Fig. S4 HRTEM images of (a) DA-Pt (1:0) and (b) DA-Pt (1:2).

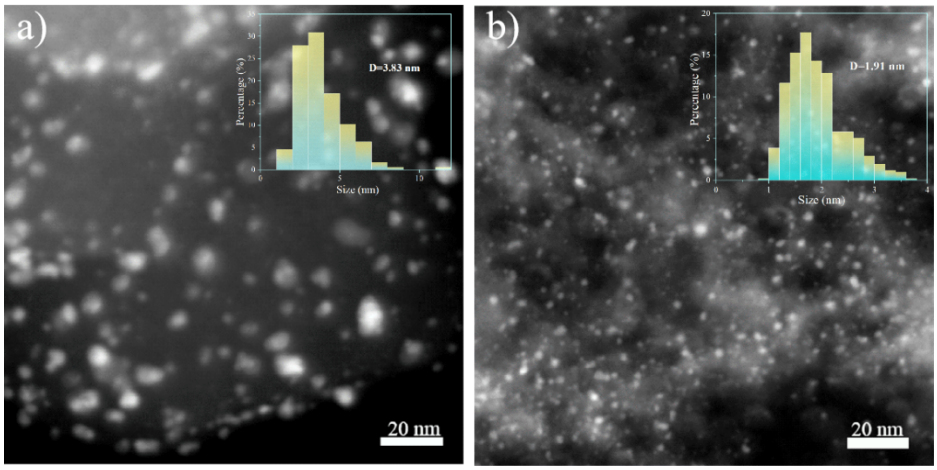

Fig. S5 Particle size distribution histograms of DA-Pt (1:0) and DA-Pt (1:2).

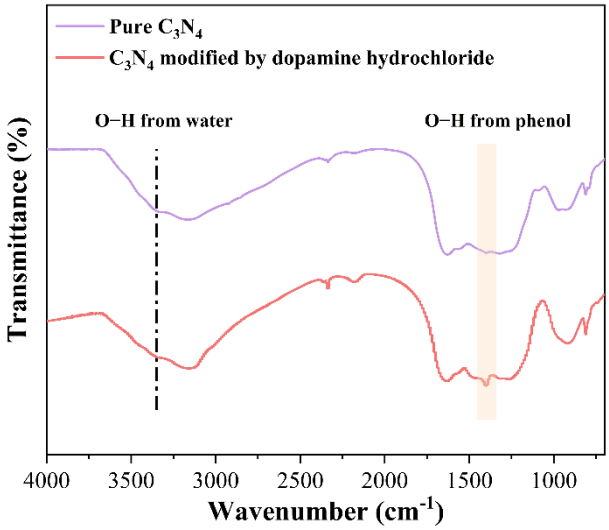

Fig. S6 FTIR spectra of pure C_3N_4 and C_3N_4 modified by dopamine hydrochloride.

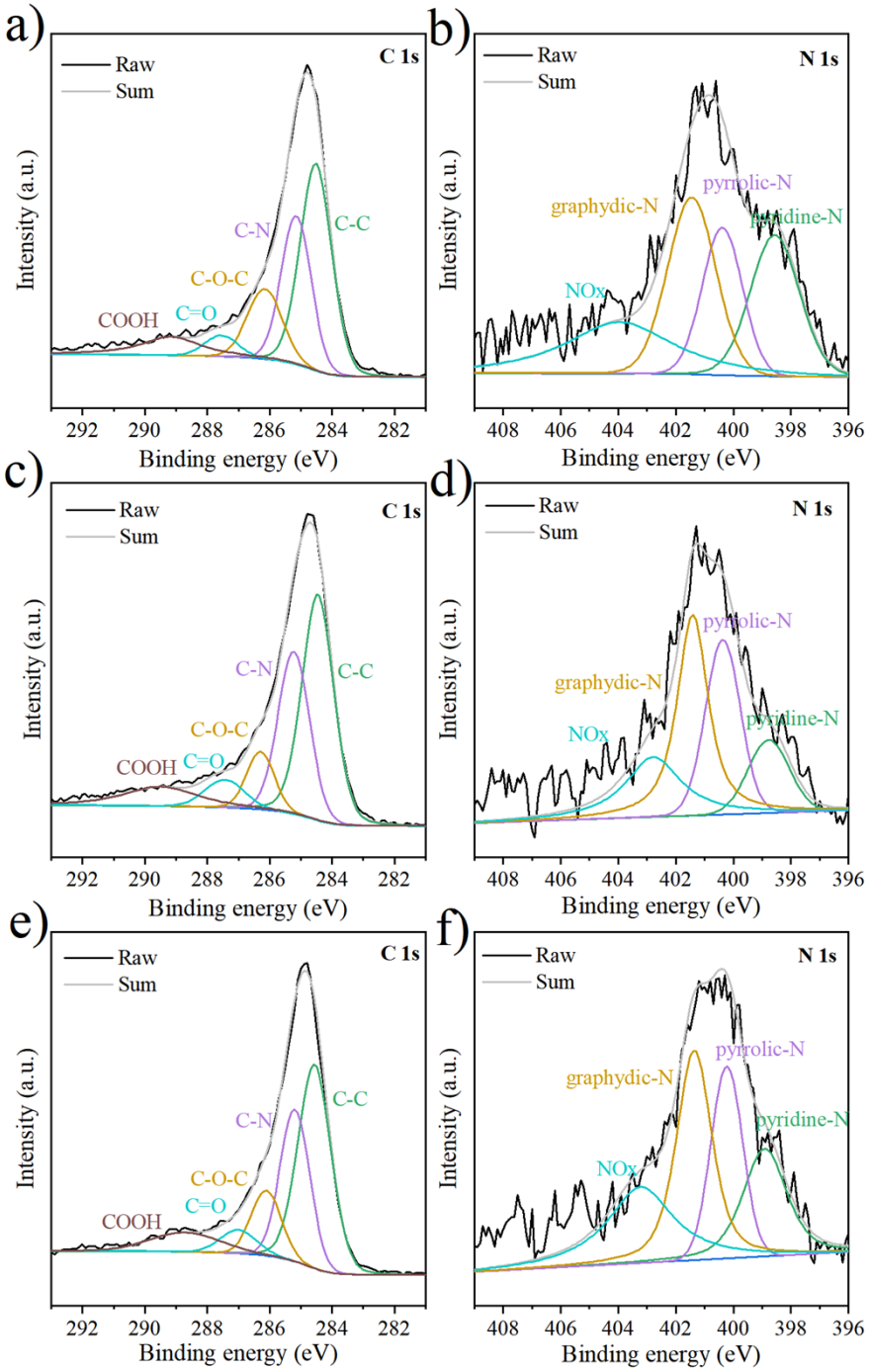

Fig. S7 High-resolution C 1s XPS spectra of (a) DA-Pt (1:0), (c) DA-Pt (1:1) and (e) DA-Pt (1:2), respectively, and N 1s XPS spectra of (b) DA-Pt (1:0), (d) DA-Pt (1:1) and (f) DA-Pt (1:2), respectively.

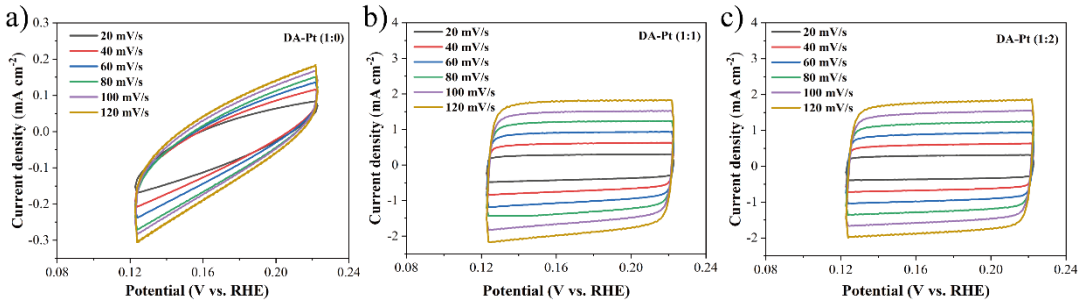

Fig. S8 CV curves at different scan rates of (a) DA-Pt (1:0), (b) DA-Pt (1:1), and (c) DA-Pt (1:2), respectively.

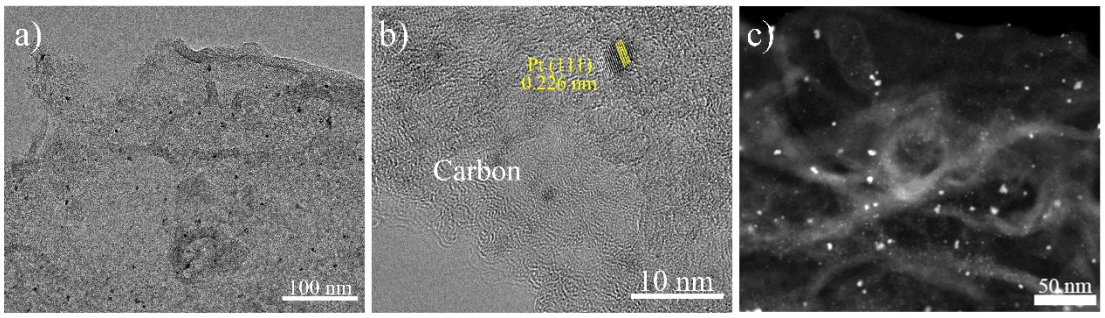

Fig. S9 (a) TEM image, (b) HRTEM micrographs corresponding lattice structure analysis and (c) HAADF-STEM of DA-Pt (1:1) after 3000 cycles.

Table. S1 List of the relative content of chemical bonds from deconvoluted N 1s XPS spectral.

Samples	pyridinic-N (%)	pyrrolic-N (%)	graphite-N (%)	oxidized-N (%)
DA-Pt (1:0)	23.92	19.27	28.15	28.66
DA-Pt (1:1)	13.20	21.49	38.75	26.56
DA-Pt (1:2)	20.00	21.03	31.89	27.08

Table S2 Comparison of HER performance of DA-Pt (1:1) catalyst with other reported electrocatalysts in 1M acidic electrolyte (0.5 M H_2SO_4).

Catalyst	Current density (mA cm^{-2})	Overpotential (mV)	Tafel	Potential (mV)	Mass activity (A g^{-1}_{Pt})	Substrate	Reference
DA-Pt (1:1)	10	17	29.1	100	5526	GC	This work
20% Pt/C	10	14	32.5	100	1400	GC	This work
Pt-HEC	10	70	47	130	1700	CC	[1]
PtW NPs/C	10	19.4	27.8	20	566.1	RDE	[2]
PtCoFe@CN	10	45	32	-	-	GC	[3]
E-MoS_2-Pt	10	29	29	50	830	GC	[4]
Pt/Ti_3C_2Tx-550	10	32.7	32.3	50	1310	CF	[5]
Pt/HPC-14.1	10	24	33	24	710	GC	[6]
Pt NP/WO_3@x	10	47	45	50	12800	RDE	[7]

Reference

1 D. Kim, S. Surendran, Y. Jeong, Y. Lim, S. Im, S. Park, J. Y. Kim, S. Kim, T. H. Kim, B. Koo, K. Jin and U. *Sim*, *Adv. Mat. Techno*, 2022, **2200882**, 2200882-2200888.

2 D. Kobayashi, H. Kobayashi, D. Wu, S. Okazoe, K. Kusada, T. Yamamoto, T. Toriyama, S. Matsumura, S. Kawaguchi, Y. Kubota, S. M. Aspera, H. Nakanishi, S. Arai and H. Kitagawa, *J. Am. Chem. Soc*, 2020, **142**, 17250-17254.

3 J. Chen, Y. Yang, J. Su, P. Jiang, G. Xia and Q. Chen, *ACS Appl. Mater. Interfaces*, 2017, **9**, 3596-3601.

4 Y. Li, S. Wang, Y. Hu, X. Zhou, M. Zhang, X. Jia, Y. Yang, B.-L. Lin and G. Chen, *J. Mater. Chem. A*, 2022, **10**, 5273-5279.

5 Z. Li, Z. Qi, S. Wang, T. Ma, L. Zhou, Z. Wu, X. Luan, F. Y. Lin, M. Chen, J. T. Miller, H. Xin, W. Huang and Y. Wu, *Nano Lett*, 2019, **19**, 5102-5108.

6 M. Song, Y. Song, H. Li, P. Liu, B. Xu, H. Wei, J. Guo and Y. Wu, *Electrochim. Acta*, 2019, **320**, 134603.

7 J. Park, S. Lee, H. E. Kim, A. Cho, S. Kim, Y. Ye, J. W. Han, H. Lee, J. H. Jang and J. Lee, *Angew. Chem., Int. Ed*, 2019, **58**, 16038-16042.